



The Selective in vitro Cytotoxicity of *Spirulina*-Derived Nanoparticles: A Novel Biomimetic Approach to Cancer Therapy

Eliyahu Drori, Valeria Rahamim, Dhaval Patel, Yamm Anker , Sivan Meir, Gal Uzan, Chen Drori, Yaakov Anker, Aharon Azagury 

Department of Chemical Engineering, Ariel University, Ariel, Israel

Correspondence: Aharon Azagury, Email aharona@ariel.ac.il

Introduction: Cancer treatment often involves significant side effects, necessitating the need for more selective therapies. *Spirulina*-derived nanoparticles (sNPs) have shown promise as a targeted anticancer strategy.

Methods: This study evaluated the cytotoxic effects of sNPs on cancer cell lines TR-146 (buccal), Caco-2 and HT-29 (colorectal), and MCF-7 (breast), compared to the non-cancerous MCF-10A cells. Cytotoxicity was assessed using the XTT assay at concentrations of 25–500 mg/mL over 3–48 hours. Cellular uptake was quantified via fluorescence-activated cell sorting (FACS) and fluorescence microscopy, and endocytic inhibitors were used to investigate the uptake mechanism.

Results: sNPs induced 30–80% mortality in cancer cells, while non-cancerous MCF-10A cells exhibited negligible mortality (<5%). Male-derived Caco-2 cells were more sensitive to sNPs than female-derived HT-29 cells, suggesting potential sex-based differences. FACS analysis showed 100% cellular uptake in all cancer cells, with TR-146 exhibiting the highest fluorescence intensity. Endocytosis inhibition studies revealed that caveolae-mediated endocytosis played a significant role in sNP uptake, particularly in TR-146 and Caco-2 cells.

Discussion: These findings demonstrate the potential of sNPs as selective and potent anticancer agents, warranting further research to optimize their clinical application.

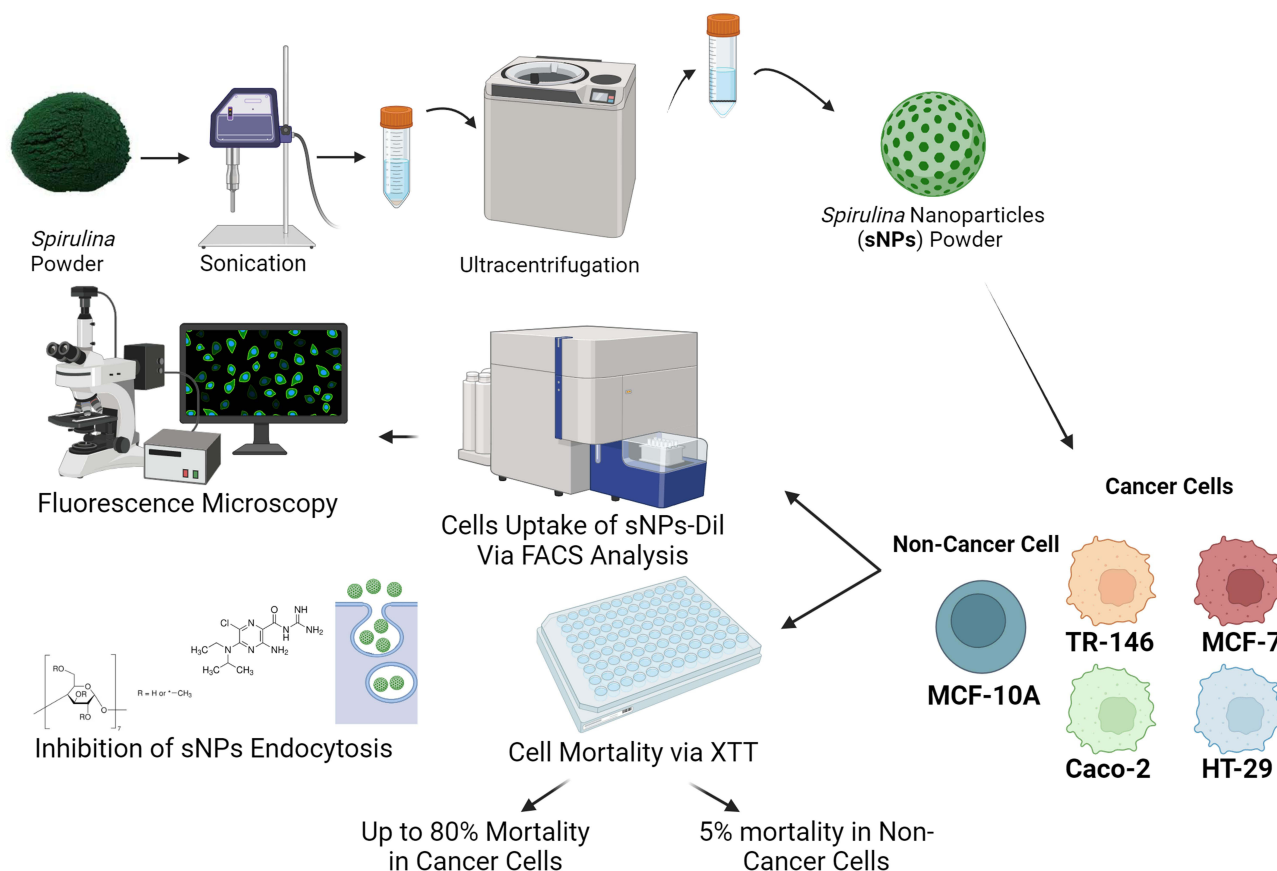
Keywords: *Spirulina*, nanoparticles, cancer therapy, biomimetics, cellular uptake, endocytic inhibitors

Introduction

Cancer treatments like chemotherapy and radiotherapy remain the cornerstone of oncological care, effectively targeting rapidly dividing cells to inhibit tumor growth and progression.¹ Nevertheless, these treatments still lack specificity, resulting in damage to healthy tissues and causing severe side effects such as immune suppression, fatigue, gastrointestinal disturbances, and hair loss.² Moreover, the emergence of drug resistance poses a significant challenge, as cancer cells can develop mechanisms to evade treatment, including increased drug efflux, alterations in drug targets, and enhanced DNA repair pathways.³ These limitations reduce the therapeutic efficacy and compromise patients' quality of life.⁴ Thus, several studies have highlighted the pressing need for innovative targeted approaches to minimize off-target effects while effectively combating cancer cells.^{5,6} Novel strategies, such as leveraging bioactive compounds from natural sources, are gaining traction as promising alternatives for addressing these challenges, offering the potential for reduced toxicity and improved treatment outcomes.⁷

Recent advances in cancer research have focused on the potential of natural compounds derived from marine organisms, such as algae, as alternative cancer treatments.⁸ Algae are rich sources of various bioactive compounds such as polysaccharides, proteins, lipids, vitamins, and antioxidants, demonstrating anti-cancer properties in multiple studies.^{9,10} Among the different types of algae, *Spirulina Platensis*, a blue-green microalga, has garnered significant attention for its potential role in cancer therapy.¹¹ *Spirulina*, particularly in whole biomass and water extracts, contains

Graphical Abstract



high levels of phycocyanin, polysaccharides, vitamins, and essential fatty acids, demonstrating immunomodulatory, anti-inflammatory, and antioxidant properties.^{11–13} Several in vitro and in vivo studies using these *Spirulina* preparations have shown that they can inhibit cancer cell proliferation, induce apoptosis, and reduce tumor growth across various cancer models.¹⁴ In a previous study, we reported the successful production of NPs derived from *Arthrospira platensis* and additional edible algae species.¹⁵ We confirmed via cryo-TEM microscopy that all the algal-based NPs exhibited a liposomal-like morphology. Specifically, sNPs showed an average diameter of 126 ± 2 nm, a polydispersity index of 0.14 ± 0.001 , and a zeta potential of -38 ± 3 mV (via DLS).¹⁵

In this study, we aim to explore the efficacy of sNPs as an anticancer and selective agent to treat cancer. To this end, we tested the effects of sNPs on several cancer cell lines: TR-146 (buccal cancer), Caco-2 and HT-29 (colorectal cancer), and MCF-7 (breast cancer) as well as on the non-cancerous cell line, MCF-10A. The cytotoxic effects of sNPs at different concentrations and exposure times using XTT assay were tested, and their cellular uptake via flow cytometry and fluorescence microscopy. Finally, we investigated the role of endocytic pathways of sNPs by employing endocytosis inhibitors. While *Spirulina* is often used as a whole cell or combined with metallic NPs, this study uniquely presents a method for producing sNPs without potentially toxic materials.

While *Spirulina* is often used as a whole cell or combined with metallic NPs, this study uniquely presents a method for producing sNPs without toxic solvents.¹⁵ In this study, we aim to explore the efficacy of sNPs as a selective anticancer agent in treating cancer. To this end, we tested the effects of sNPs on several cancer cell lines: TR-146 (buccal cancer), Caco-2 and HT-29 (colorectal cancer), and MCF-7 (breast cancer) as well as on the non-cancerous cell line, MCF-10A. The cytotoxic effects of sNPs were assessed at different concentrations and exposure times using the XTT

assay, and their cellular uptake was analyzed via flow cytometry and fluorescence microscopy. Finally, we investigated the role of endocytic pathways in sNP internalization by employing endocytosis inhibitors.

Materials and Methods

Materials

The cell lines MCF-10A, MCF-7, Caco-2, HT-29, and TR-146 were obtained from ATCC®. Growth media, supplements, and materials were sourced as follows: DMEM/F12, DMEM, L-Glutamine, and Penicillin-Streptomycin from Sartorius Israel; human Insulin, Cholera Toxin, Hydrocortisone, Epidermal Growth Factor, Trypsin-EDTA, Phosphate-buffered saline (PBS), FBS, sucrose, MβCD, 5-(N-ethyl-N-isopropyl) amiloride (EIPA), XTT assay kits, Dil dye, DAPI, and paraformaldehyde from Sigma-Aldrich Israel. *Spirulina* powder was purchased from NutriCargo, USA.

Harvesting sNPs

To produce sNPs, 0.6 g of *Spirulina* powder was mixed with 240 mL of double-distilled water and sonicated (Q700, Qsonica) in an ice bath at 100% amplitude and 50% duty cycle for 2 minutes. The suspension was centrifuged at $3,200 \times g$ for 5 minutes at 4°C, and the supernatant underwent additional sonication and centrifugation. The refined supernatant was further centrifuged at $10,000 \times g$ for 60 minutes at 4°C, transferred onto a 60% sucrose layer, and ultracentrifuged at $150,000 \times g$ for 45 minutes at 4°C. The sNPs solution was extracted, frozen at −80°C, lyophilized (Labconco FreeZone 4.5 L), and stored in powder form.¹⁵

Evaluation of sNPs Impact on Cell Mortality

The cell lines MCF-10A, MCF-7, Caco-2, HT-29, and TR-146 were cultured in their respective growth media under standard conditions. Cells were maintained in a humidified incubator at 37°C with 5% CO₂ and were subcultured upon reaching 70–80% confluency. The cells were cultured in a 96-well plate (Greiner, Monroe, NC, USA), seeding approximately 8,000 cells per well to obtain 70–80% confluency after 24 h of incubation. Before incubation with the cells, the sNP solutions were filtered to ensure sterility using a 0.22 μm PVDF-membrane syringe filter (Romical Israel). The filtered sNPs were then diluted with the growth medium to various concentrations (25, 50, 125, 250, 375, and 500 mg/mL), and 100 μL of this solution was added to the cells. The tested incubation times were 3, 6, 12, 24, and 48 h.

The XTT assay¹⁶ was used to evaluate cell viability, following standard preparation and incubation protocol.¹³ Absorbance was measured at a wavelength of 500 nm using a microplate reader (Infinite M200 Tecan). The mortality rate for each cell type was calculated in comparison to the control group (cells cultured with growth medium only).

Examining Endocytosis of sNPs in Cell Lines

To assess if endocytosis plays a part in the sNP toxicity mechanism, the cells were exposed to two inhibitors—40 μM MβCD and 10 mM EIPA—and incubated at 37°C for 40 min. Following this incubation, 100 μL of sNPs (125 and 500 mg/mL) were added to each well.¹⁴ Finally, cell mortality was evaluated using the XTT assay as described above.

Preparation of Dil-Labeled sNPs

sNPs were labeled with a fluorescent lipophilic dye, Dil, to assess cellular uptake. A 0.1 mg/mL Dil solution (100 μL) was added to 10 mL of 500 mg/mL sNPs, followed by incubation for 30 minutes at 37°C. The Dil-labeled sNPs were then purified by ultrafiltration at $150,000 \times g$ for 45 minutes at 4°C, and the pellet was collected for further experimentation.

Evaluation of Cellular Uptake by Flow Cytometry and Fluorescence Microscopy

The cell lines MCF-10A, MCF-7, Caco-2, HT-29, and TR-146 were seeded in a 6-well plate (Greiner, Monroe, NC, USA) at a density of 1×10^5 cells per well and cultured overnight at 37°C until they reached 70–80% confluence. The culture medium was then replaced with fresh medium containing 500 μg/mL Dil-labeled sNPs, and the cells were incubated for an additional 3 hours to allow for uptake. After this incubation, the cells were washed twice with PBS, and

1 mL of trypsin containing 300 nM DAPI was added to each well for 10 minutes to detach the cells. The cells were centrifuged at $500 \times g$ for 12 minutes, and the pellet was collected. The cells were fixed with 4% PFA and transferred to a 96-well plate on ice. FACS instrument (CytoFLEX Beckman Coulter, Indianapolis, IN, USA) was then performed to quantitatively assess the uptake and Mean fluorescence intensity (MFI) of Dil-labeled sNPs.¹⁷

To further confirm the cellular uptake of sNPs, TR-146 buccal cancer cells were incubated with 500 $\mu\text{g/mL}$ Dil-labeled sNPs for 3 hours. Following incubation, the cells were washed with PBS, fixed with 4% PFA, and stained with DAPI to visualize the nuclei. The cells were then transferred onto a glass slide for fluorescence microscopy (Olympus™ CKX53) analysis. Images were captured to observe the red fluorescence from the Dil-labeled sNPs and the blue fluorescence from the DAPI-stained nuclei. The captured fluorescence images were processed for qualitative analysis using ImageJ version ij154 software. The red (Dil-labeled sNPs) and blue (DAPI-stained nuclei) channels were merged to confirm the co-localization of sNPs within the TR-146 cells.

Statistical Analysis

GraphPad Prism (version 10) was used to analyze the data. The Shapiro–Wilk test was applied to check data normality, while the Brown–Forsythe test assessed the homogeneity of variances. Group differences were evaluated using a one-way ANOVA analysis with Fisher’s Least Significant Difference (LSD) post hoc test at $\alpha = 0.05$. A one-way ANOVA analysis with Dunnett was used to compare one variable. Presented values are the mean \pm standard deviation (SD) of a minimum of $n = 3$ per condition. The Median Lethal Concentration (LC_{50}) values were calculated using non-linear regression analysis (log(inhibitor) vs response – variable slope) with GraphPad Prism, fitting the concentration-response data to determine the concentration of sNPs required to inhibit 50% of cell viability.

Results and Discussion

Evaluation of sNPs Impact on Cell Mortality

The cytotoxic effects of sNPs were evaluated, and the results are presented in [Figures 1–5](#) for the cell lines TR-146, Caco-2, HT-29, MCF-7, and MCF-10A, respectively. A statistical test was performed comparing all groups against the selected concentration at each time point, where this concentration represented the one that resulted in the highest observed mortality. Concentrations above this level showed no significant increase in mortality, while concentrations below it demonstrated a statistically significant difference.

The cytotoxic effects of sNPs were evaluated on various cancer cell lines ([Figures 1–5](#)). TR-146 buccal cancer cells showed the highest mortality (~80%) primarily at 125 mg/mL sNPs across all exposure times, with no further increase at higher concentrations ([Figure 1](#)). Caco-2 cells required higher sNP concentrations (250–375 mg/mL) to reach similar mortality (~80%), with increased exposure time or concentrations having no significant effect ([Figure 2](#)). HT-29 cells also demonstrated the highest mortality at 250–375 mg/mL, although extended incubation appeared to increase the mortality rate slightly. However, their peak mortality (~70%) was lower than TR-146 and Caco-2 cells ([Figure 3](#)). The MCF-7 breast cancer cells were less affected by sNPs, achieving a maximum mortality of 65%, and exhibited the strongest correlation to both concentration and exposure time, reaching peak mortality at 125 mg/mL after 48 hours ([Figure 4](#)). In contrast, the noncancerous MCF-10A cells showed no statistically significant cytotoxic effects across all concentrations and exposure times ([Figure 5](#)). These results strongly suggest that sNPs have selective toxicity towards cancerous cells, offering promising potential for targeted cancer therapy. Overall, exposing cancerous cells to sNPs resulted in a dose- and time-dependent increase in mortality, ranging from approximately 30% to 80%.

Additionally, the cytotoxic effect of sNPs on Caco-2 cells has been documented, showing that it can significantly reduce cell viability through several mechanisms. Śmieszek et al¹⁸ demonstrated that *Spirulina platensis* filtrates (SPF) exert strong anti-proliferative and pro-apoptotic effects on Caco-2 cells, impacting cell morphology, inhibiting metabolic activity, and decreasing pro-survival gene expression. Unlike these studies that used whole-cell extracts, our study utilized sNPs produced without cytotoxic agents such as ethanol or methanol. Cryo-TEM imaging indicated that these sNPs have a liposomal-like structure,¹⁵ which could enhance their cellular uptake and bioavailability. This suggests that

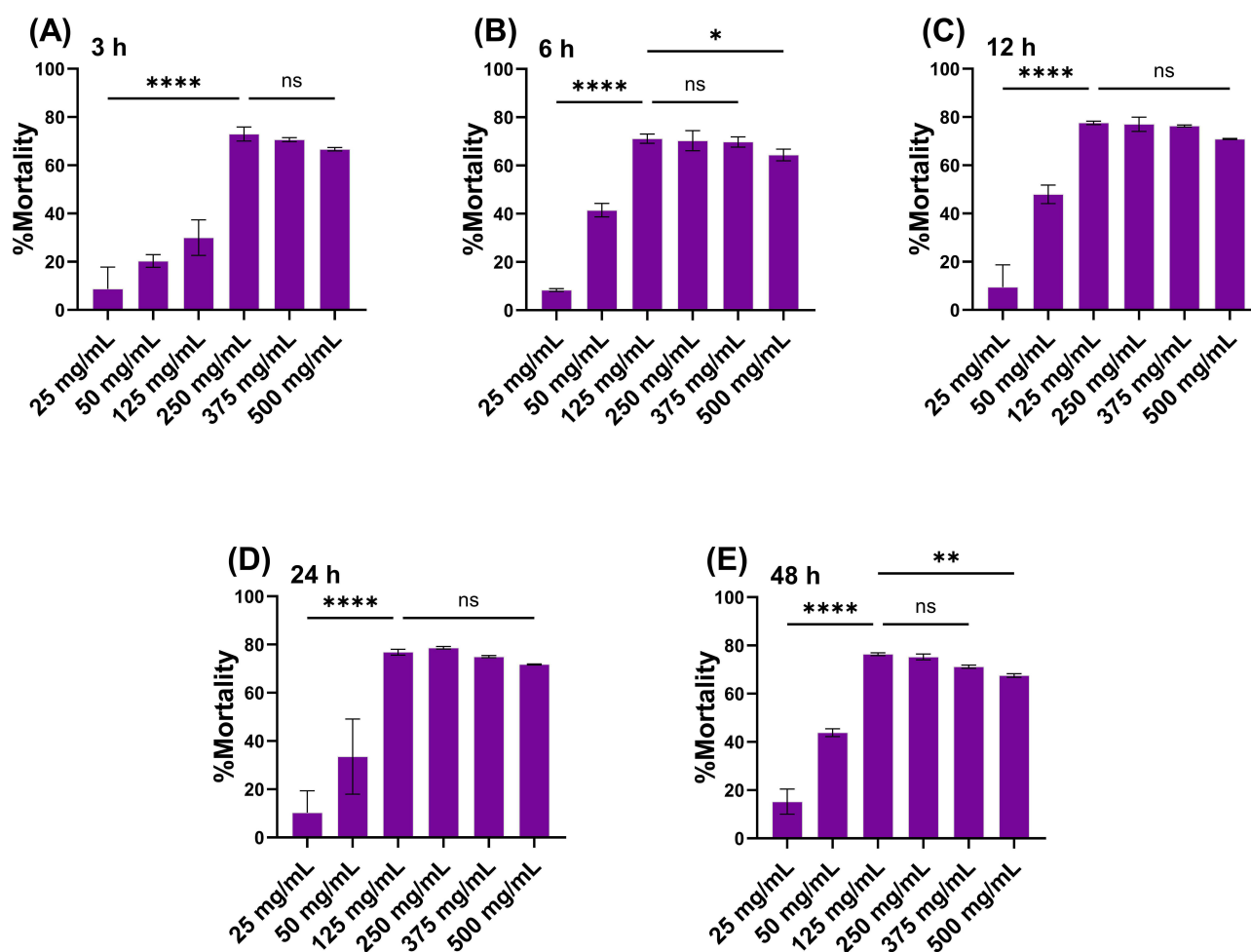


Figure 1 Percentage of mortality in TR-146 cells exposed to sNPs concentrations of 25, 50, 125, 250, 375, and 500 mg/mL for (A) 3 h, (B) 6 h, (C) 12 h, (D) 24 h, and (E) 48 h. Statistical significance was assessed using one-way ANOVA with Dunnett's post hoc test, comparing each concentration against the concentration showing the highest mortality at each time point. Values represent the mean \pm SD from at least three independent experiments. Statistical significances are denoted as * $p < 0.05$, ** $p < 0.01$, *** $p < 0.0001$, and ns for non-significant.

sNPs offer a more efficient and targeted approach, demonstrating selective cytotoxicity, particularly towards TR-146 and Caco-2 cancer cell lines.

Recent studies have further highlighted the potential of *Spirulina* in cancer therapy. For instance, silver NPs synthesized using *Spirulina platensis* phycocyanin exhibited significant anticancer activity against lung (A-549) and breast (MCF-7) cancer cell lines, demonstrating their effectiveness as therapeutic agents.¹⁹ Similarly, biogenic silver chloride NPs produced from *Spirulina platensis* extracts showed strong cytotoxic effects against MDA-MB231 breast cancer cells, emphasizing their ability to induce apoptosis in cancer cells.²⁰ These findings align with our results, as the sNPs in this study demonstrated selective cytotoxicity towards TR-146 and Caco-2 cells. However, a key advantage of our approach is that the sNPs in this study were produced without the addition of cytotoxic agents or surface functionalization, achieving high cytotoxicity levels solely through the inherent properties of sNPs.

To further assess the effect of exposure time of cancerous and noncancerous cells to sNPs, we plotted the calculated LC_{50} using GraphPad Prism for all the cells (Figure 6). Note that no LC_{50} values are presented for MCF-10A cells since no significant mortality was observed.

Figure 6 presents the dependency of LC_{50} values for the tested cell lines on exposure times. As expected, all the tested cells exhibited a decrease in LC_{50} values over time, indicating increased sensitivity to sNPs with prolonged exposure. For three h exposure, MCF-7 cells showed the highest LC_{50} value of around 400 mg/mL, demonstrating the lowest sensitivity to sNPs, but this value significantly decreased over time (<200 mg/mL). TR-146 cells consistently displayed the lowest

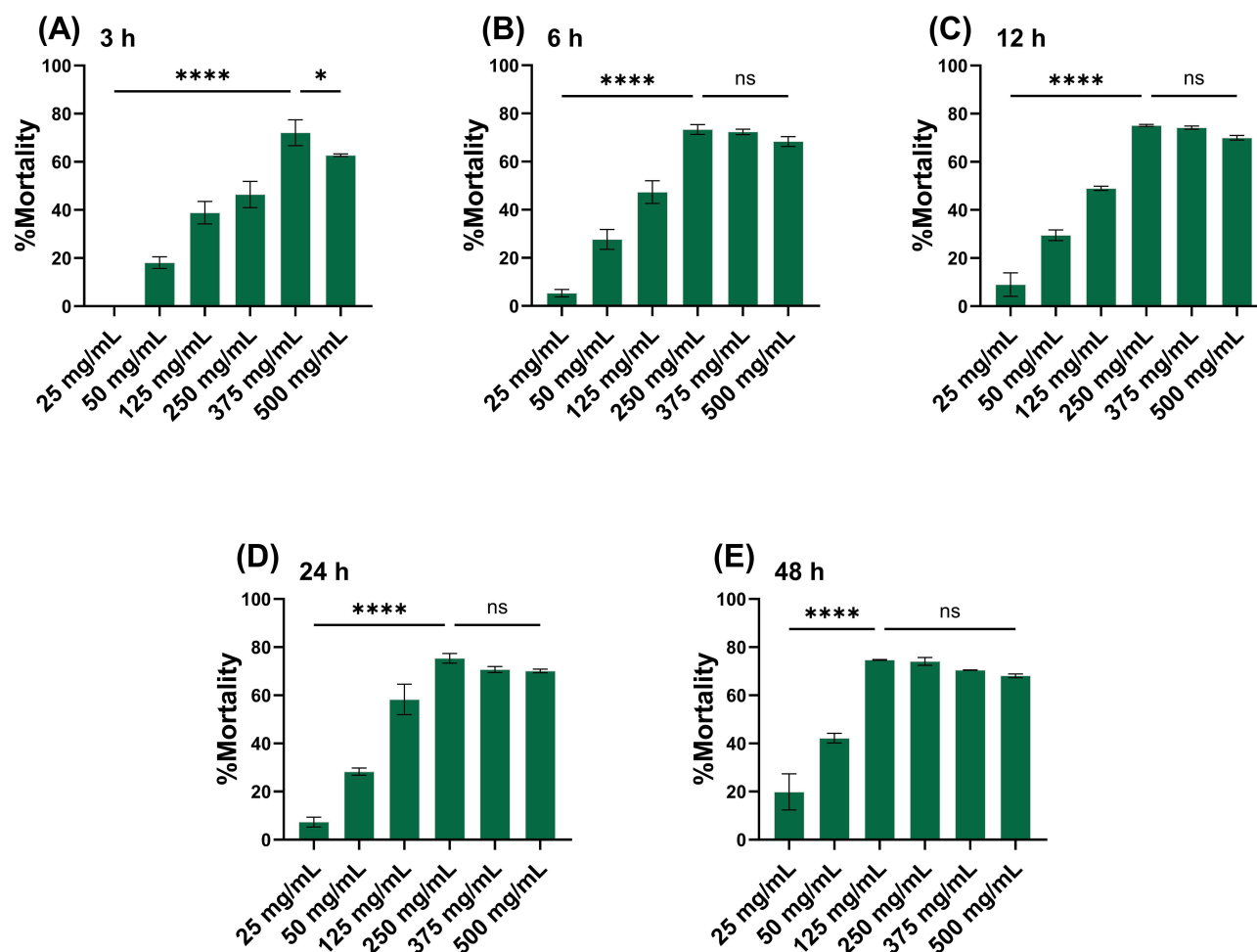


Figure 2 Percentage of mortality in Caco-2 cells exposed to sNPs concentrations of 25, 50, 125, 250, 375, and 500 mg/mL for (A) 3 h, (B) 6 h, (C) 12 h, (D) 24 h, and (E) 48 h. Statistical significance was assessed using one-way ANOVA with Dunnett's post hoc test, comparing each concentration against the concentration showing the highest mortality at each time point. Values represent the mean \pm SD from at least three independent experiments. Statistical significances are denoted as * $p < 0.05$, **** $p < 0.0001$, and ns for non-significant.

LC₅₀ values across all exposure times, indicating the highest sensitivity to sNPs. As mentioned, the LC₅₀ for the non-cancerous MCF-10A cells could not be calculated, as minimal cell death was observed across all concentrations and time points, highlighting the selective cytotoxicity of sNPs towards cancerous cells.

Notably, a difference was observed in sensitivity between the colorectal cancer cell lines, with Caco-2 cells (derived from a male) being more sensitive to sNPs than HT-29 cells (derived from a female). This increased sensitivity of Caco-2 cells may be attributed to sex-based differences in cancer, which can result from a combination of genetic and epigenetic factors, as well as differences in gene regulation and expression.²¹ Additionally, research has identified variations in the expression of μ RNAs, autophagy, apoptosis, and the activation of the X chromosome, which may contribute to the observed disparities in response to sNPs treatment between male and female-derived colorectal cancer cells.²²

To address concerns about potential delayed cytotoxicity or off-target effects, follow-up assessments were conducted for one-week post-exposure to sNPs at the highest tested concentration (500 mg/mL). After a recovery period of seven days under standard culture conditions, no statistically significant changes in cell viability were observed across all tested cell lines compared to initial results. These findings indicate that the minimal cytotoxicity observed in non-cancerous cells is not associated with delayed or off-target effects, further supporting the selective and sustained cytotoxic potential of sNPs toward cancerous cells.

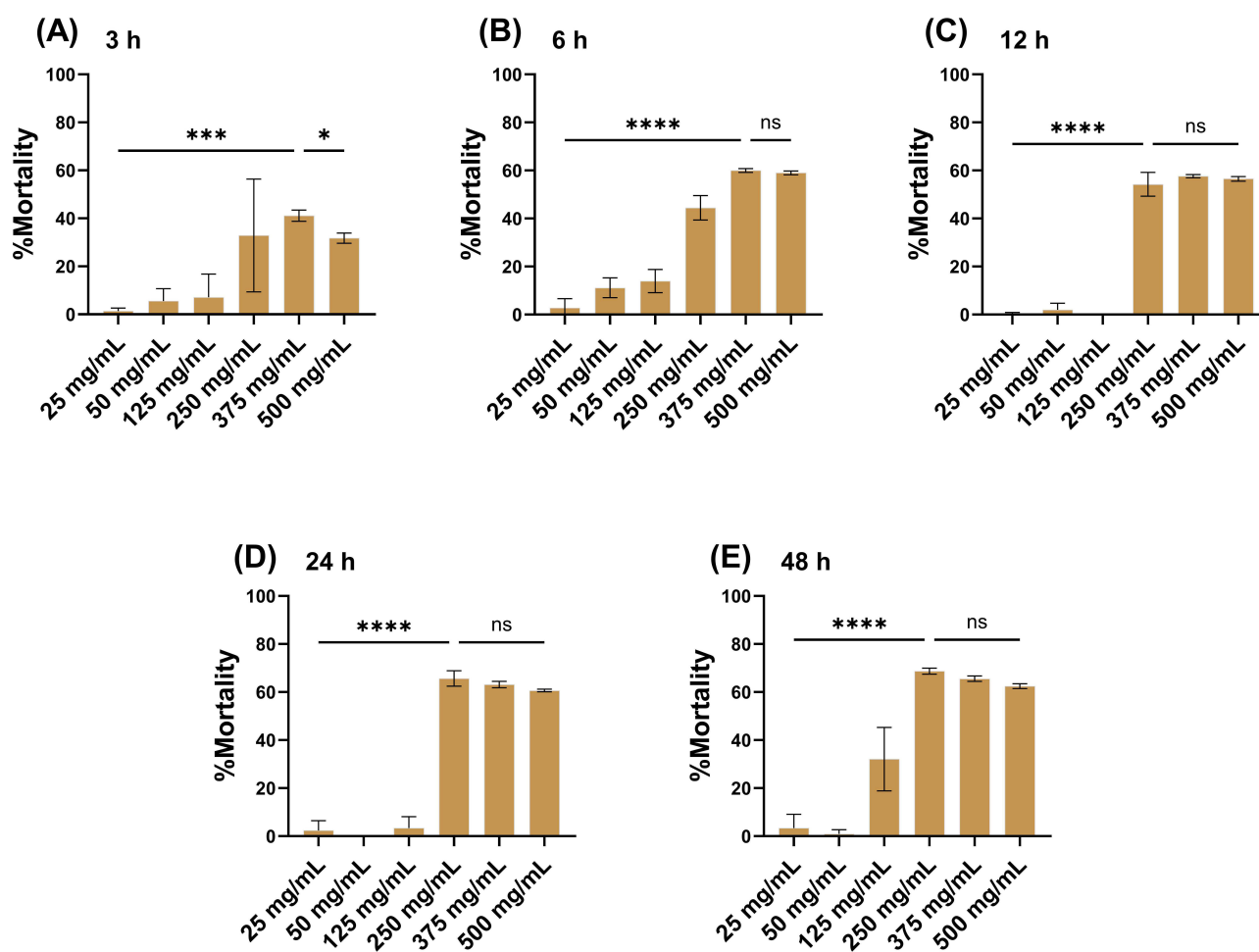


Figure 3 Percentage of mortality in HT-29 cells exposed to sNPs concentrations of 25, 50, 125, 250, 375, and 500 mg/mL for (A) 3 h, (B) 6 h, (C) 12 h, (D) 24 h, and (E) 48 h. Statistical significance was assessed using one-way ANOVA with Dunnett's post hoc test, comparing each concentration against the concentration showing the highest mortality at each time point. Values represent the mean \pm SD from at least three independent experiments. Statistical significances are denoted as * $p < 0.05$, *** $p < 0.001$, **** $p < 0.0001$, and ns for non-significant.

Evaluation of Cellular Uptake by Flow Cytometry and Fluorescence Microscopy

Following the investigation of the cytotoxic effects of sNPs on different cell lines, the next step was to evaluate the cellular uptake of these NPs by cancerous and non-cancerous cells using flow cytometry. The goal was to determine whether the differences in mortality rates result from different penetration rates. The results are presented in Table 1 below.

The most prominent result in Table 1 is that all cancerous cells showed 100% cellular uptake, while the noncancerous cells (ie, MCF-10A) showed only 60% cellular uptake after three h of exposure. This observation may also partially account for the selective toxicity of sNPs towards cancerous cells. Moreover, it suggests that sNPs need to penetrate the cells to be effective. Nevertheless, even though all cancerous cells exhibited 100% cellular uptake, the extent of penetration, indicated by the MFI parameter, varied between the different cancer cells. TR-146 buccal cancer cells showed the highest MFI (12,222), followed by the MCF-7 breast cancer cells with an MFI of 7,509, almost 40% less. The Caco-2 and HT-29 colorectal cancer cells displayed significantly lower MFIs (>75% less compared to TR-146) of 2,883 and 2,819, respectively (with 100% cellular uptake). Interestingly, a correlation was observed when examining the corresponding mortality rate. The TR-146 (67%) cells, with the highest MFI, also demonstrated the highest mortality, while the Caco-2 (62%) and HT-29 (32%) cells, with the lowest MFIs, showed comparatively lower mortality rates. This suggests that the selective cytotoxicity of sNPs is closely related to their ability to penetrate the cells, with higher internalization leading to more significant toxicity.

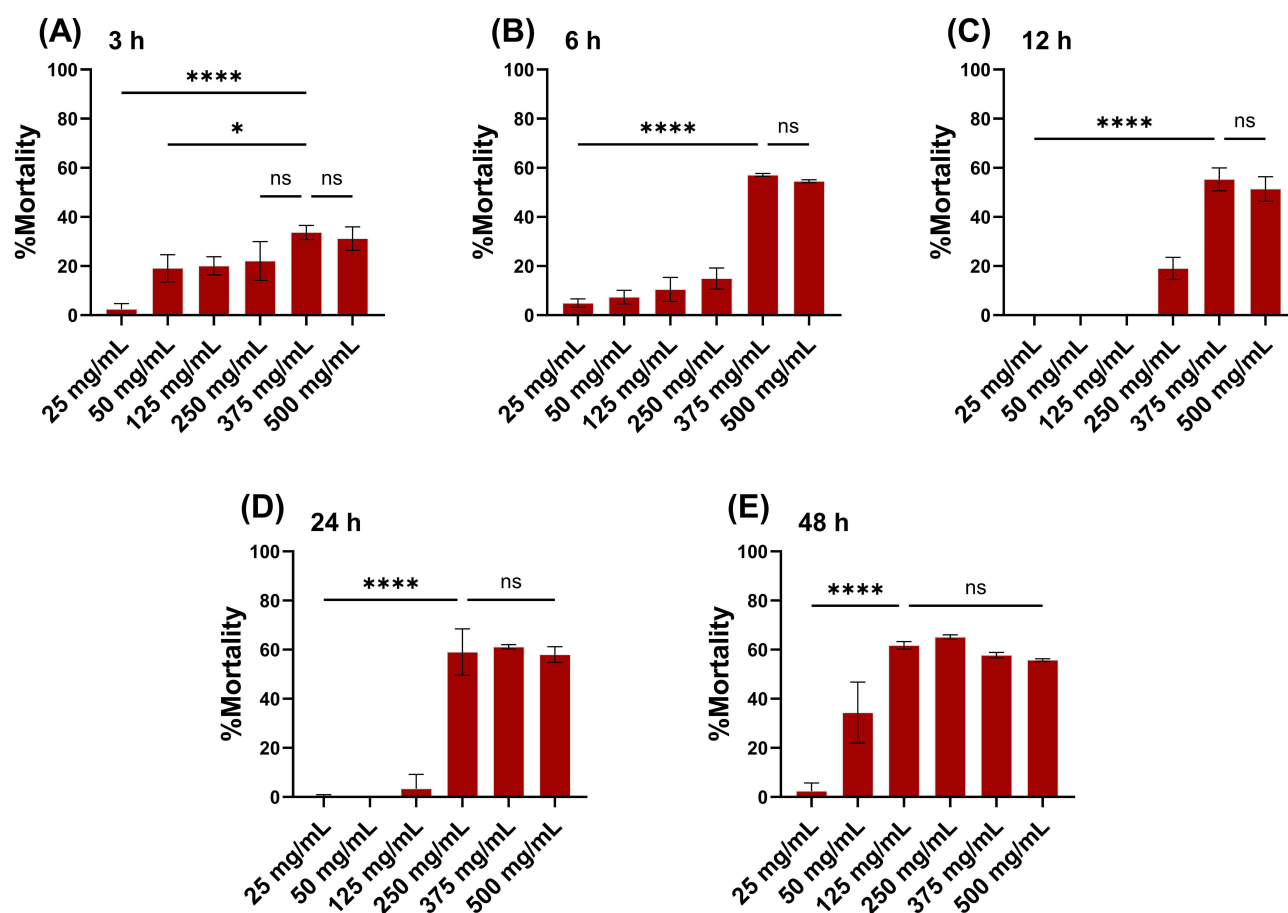


Figure 4 Percentage of mortality in MCF-7 cells exposed to sNPs concentrations of 25, 50, 125, 250, 375, and 500 mg/mL for (A) 3 h, (B) 6 h, (C) 12 h, (D) 24 h, and (E) 48 h. Statistical significance was assessed using one-way ANOVA with Dunnett's post hoc test, comparing each concentration against the concentration showing the highest mortality at each time point. Values represent the mean \pm SD from at least three independent experiments. Statistical significances are denoted as * $p < 0.05$, **** $p < 0.0001$, and ns for non-significant.

In contrast, the non-cancerous MCF-10A cells showed lower uptake, with an MFI of 2,749. Interestingly, this MFI value is similar to that observed for the cancerous HT-29 and Caco-2 cells. Even though the cellular uptake into MCF-10A was lower than in these cancerous cells, still no mortality post-incubation with sNPs was observed in the healthy cells of MCF-10A.

Furthermore, the FACS analysis highlights the difference in the cellular uptake of sNPs into cancerous and noncancerous cells. The higher fluorescence intensity observed in cancerous cells suggests a preferential interaction of sNPs with cancer cell membranes. This selective cellular uptake may be attributed to the unique characteristics of cancer cells, such as altered membrane composition or increased affinity to NPs interactions.²³ Despite similar cellular uptake (ie, 100%), the variation in MFI among the tested cancerous cell lines points to differences in the extent of NPs interactions with the cells' membranes. In conclusion, these findings reinforce the potential of sNPs to selectively target cancer cells.

This preferential uptake by cancerous cells aligns with previous studies demonstrating that NPs tend to accumulate more in cancer cells due to their higher endocytic activity and altered metabolism. This observation could be attributed to cancer cells increased endocytic activity compared to normal cells.²⁴ For example, a study by Wang et al²⁵ showed that cancer cells internalized silica nanoparticles more effectively than normal cells, resulting in increased cytotoxicity in cancerous tissues. Furthermore, in a previous study, sNPs demonstrated mucoadhesive properties to mouse small intestine tissue,¹⁵ which could enhance their residence time in the target area,²⁶ further supporting their therapeutic potential.

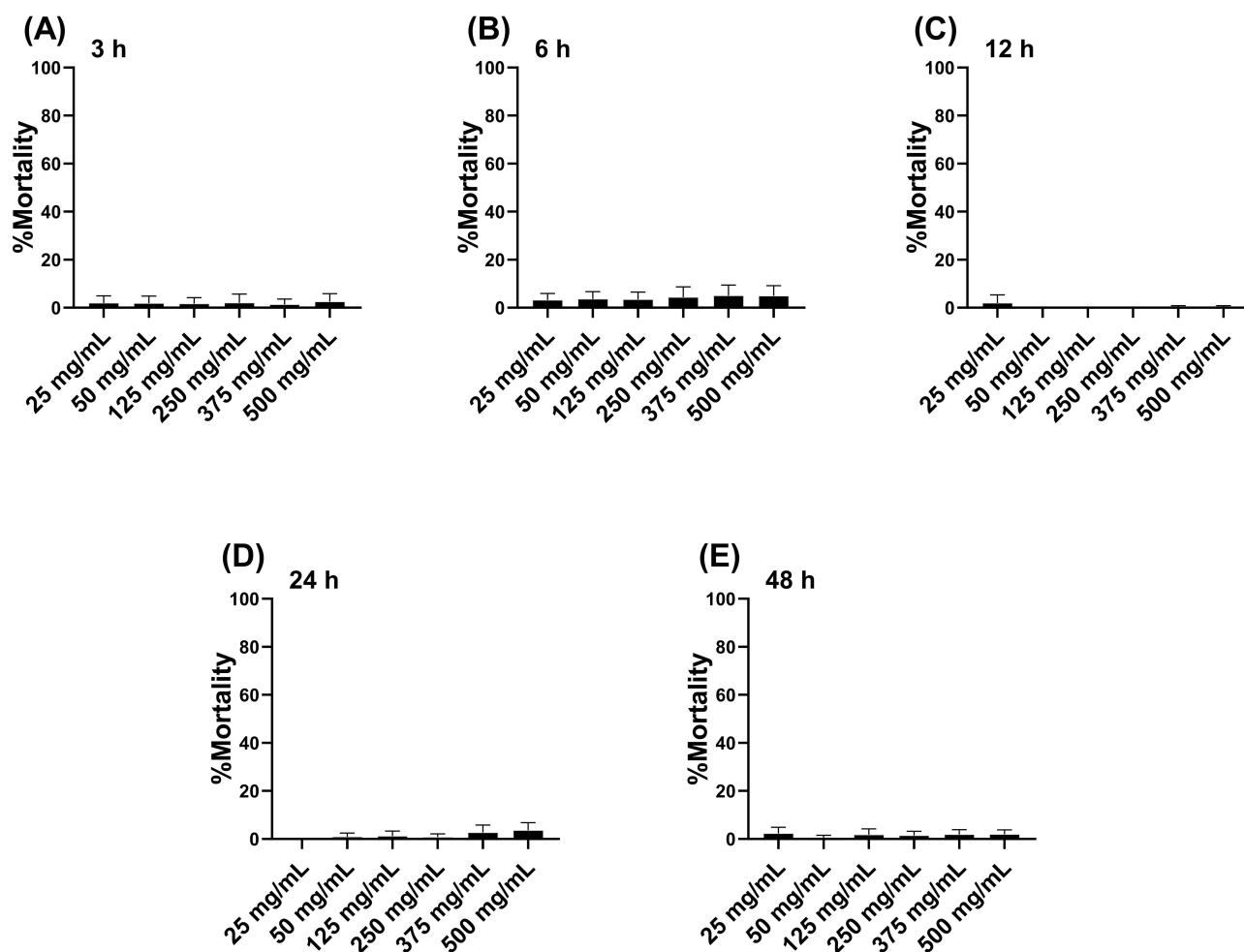


Figure 5 Percentage of mortality in MCF-10A cells exposed to sNPs concentrations of 25, 50, 125, 250, 375, and 500 mg/mL for (A) 3 h, (B) 6 h, (C) 12 h, (D) 24 h, and (E) 48 h. Statistical significance was assessed using one-way ANOVA with Dunnett's post hoc test, comparing each concentration against the concentration showing the highest mortality at each time point. Values represent the mean \pm SD from at least three independent experiments.

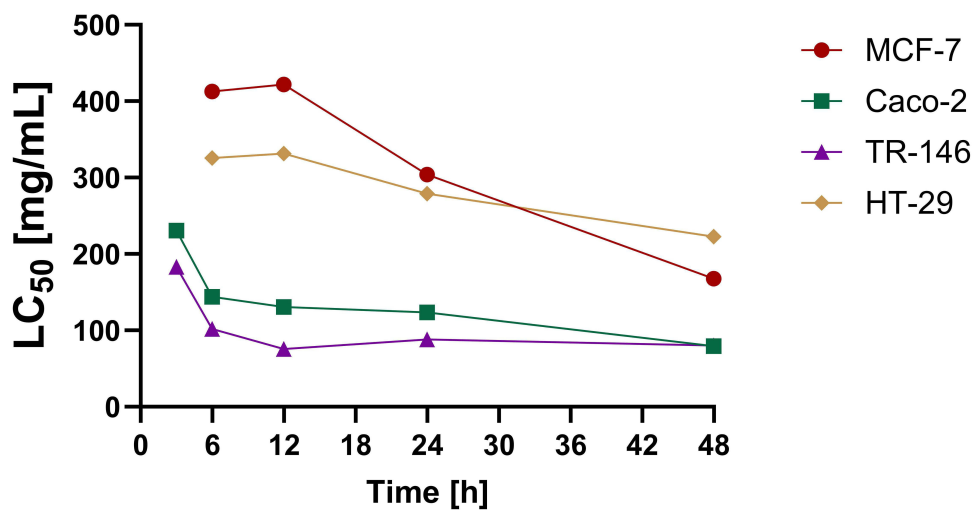


Figure 6 Presents the LC_{50} values of the different cell lines (MCF-7, Caco-2, TR-146, and HT-29) at various time points over 48 hours.

Table 1 Mean Fluorescence Intensity (MFI) and Percentage Uptake of 500 mg/mL of Dil-Labeled sNPs Into TR-146, Caco-2, MCF-7, HT-29, and MCF-10A After 3 hours of Exposure. The MFI Values Represent the Added Fluorescence Intensity in Cells Exposed to sNPs Over the Autofluorescence Intensity

Cell Line	MFI	Uptake
TR-146	12,222	100%
Caco-2	2883	100%
MCF-7	7509	100%
HT-29	2819	100%
MCF-10A	2749	60%

To visually confirm the internalization of sNPs by cancer cells, fluorescence microscopy was performed on TR-146 buccal cancer cells rather than mere surface adhesion. The sNPs were labeled with the fluorescent dye DiI, enabling us to track their penetration and localization within the cells. The DAPI stain was used to visualize the cell nuclei, confirming that the sNPs had been internalized and were not simply attached to the cell membrane (Figure 7).

The fluorescence microscopy images confirm the cellular uptake of sNPs by TR-146 buccal cancer cells. The first image shows sNPs labeled with the fluorescent dye DiI (appearing in red), indicating the presence of sNPs in proximity to the cells. The second image highlights the nuclei of the TR-146 cells stained with DAPI (in blue), showing the cellular structure. In the merged image, the overlap of the red signal from the DiI-labeled sNPs and the blue signal from the DAPI-stained nuclei demonstrates that the sNPs have been internalized or attached by the TR-146 cells. This overlap confirms that the sNPs are present within the cellular boundaries.

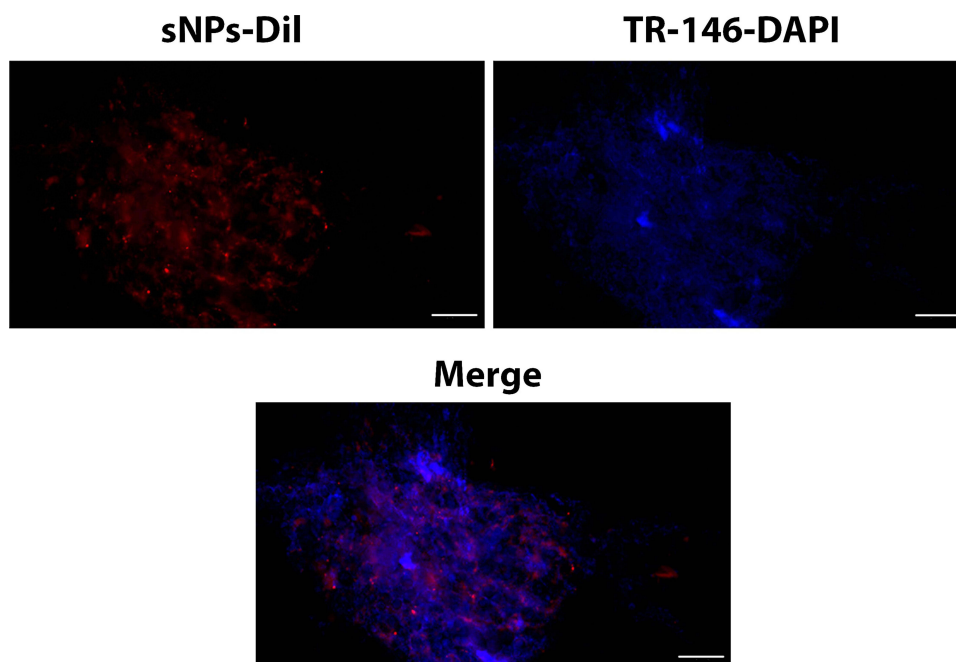


Figure 7 Fluorescence microscopy images showing the uptake of sNPs labeled with DiI (red) by TR-146 buccal cancer cells. The top left image shows the DiI-labeled sNPs (red), the top right image displays the DAPI-stained nuclei of TR-146 cells (blue), and the bottom image is a merged overlay showing the internalization of sNPs within the cells, as evidenced by the overlap of red and blue signals. Scale bars represent 100 μ m.

Assessment of Endocytosis Pathways of sNPs

Given that our and previous results from the literature suggest that the observed differences in sNPs uptake might be attributed to variations in endocytic activity, we investigated the endocytic activity of sNPs uptake. Endocytosis is a primary pathway through which cells internalize NPs, and inhibiting specific pathways can help identify how sNPs are internalized by cancerous and non-cancerous cells. To explore this, we used two inhibitors: M β CD, which disrupts caveolae-mediated endocytosis by removing cholesterol from cell membranes, and EIPA, a macropinocytosis inhibitor. The impact of these inhibitors on sNPs uptake was evaluated for the cell lines of TR-146, Caco-2, HT-29, MCF-7, and MCF-10A (Figure 8).

For the MCF-7 breast cancer cells (Figure 8A), blocking caveolae-mediated endocytosis with M β CD resulted in a statistically significant decrease in mortality from 31% to 19% at the 500 mg/mL concentration ($p < 0.05$), suggesting that caveolae-mediated endocytosis is crucial for sNPs uptake in these cells and induced toxicity. No significant effects were seen at 125 mg/mL, likely due to the lower quantity of NPs at this concentration, nor with EIPA treatment, indicating that macropinocytosis does not play a role in sNPs uptake to MCF-7 cells. The non-cancerous MCF-10A cells (Figure 8B) showed no significant changes in mortality at both concentrations with M β CD or EIPA, indicating that these endocytosis pathways do not impact sNPs uptake or cytotoxicity, consistent with the lower uptake and mortality rates observed in these cells.

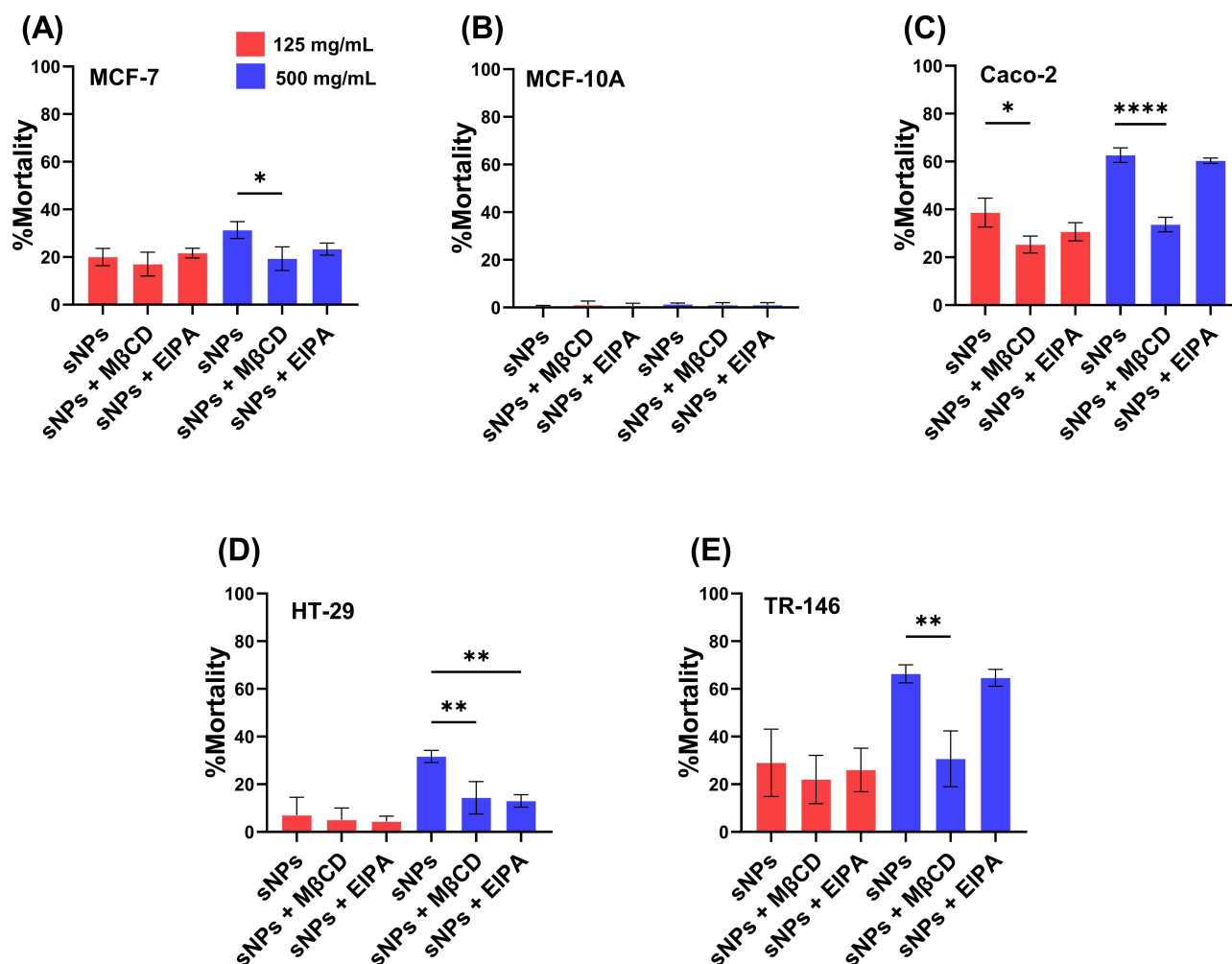


Figure 8 The impact of endocytosis inhibitors (M β CD and EIPA) on the uptake of sNPs into the cell lines (A) TR-146, (B) Caco-2, (C) HT-29, (D) MCF-7, and (E) MCF-10A. Values represent the mean \pm SD from at least three independent experiments. Statistical analysis was performed using one-way ANOVA followed by Fisher's LSD post hoc test, with significance indicated as follows: * $p < 0.05$, ** $p < 0.01$, and **** $p < 0.0001$.

Different patterns emerged for the colorectal cancer cell lines. In the Caco-2 cells (Figure 8C), a significant reduction in mortality from 39% to 25% was observed with M β CD treatment at 125 mg/mL ($*p < 0.05$) and 500 mg/mL ($****p < 0.0001$) from 63% to 34%, suggesting that caveolae-mediated endocytosis is the dominant pathway for sNPs uptake in these cells. In contrast, EIPA treatment had no significant effect, highlighting that macropinocytosis is not a major route for sNPs internalization in Caco-2 cells. This aligns with their increased mortality rates and correlates with earlier results showing high sNPs uptake in Caco-2 cells.¹⁵ In HT-29 colorectal cancer cells (Figure 8D), a statistically significant decrease in mortality from 32% to 14% was observed at 500 mg/mL with M β CD ($**p < 0.01$) and EIPA treatments from 32% to 13%, suggesting that both caveolae-mediated endocytosis and macropinocytosis contribute to sNPs uptake to HT-29. Finally, in TR-146 buccal cancer cells (Figure 8E), M β CD treatment at 500 mg/mL resulted in a significant reduction in mortality from 66% to 31% ($**p < 0.01$), suggesting that caveolae-mediated endocytosis is a significant pathway for sNPs uptake in these cells. No significant effect was observed with EIPA treatment.

A comparison between Caco-2 and HT-29 cells (Figure 8C and D) reveals again sex-based differences in endocytosis, as Caco-2 cells responded significantly only to M β CD, whereas HT-29 cells responded to M β CD and EIPA. This suggests that variations in cholesterol metabolism and endocytic pathways might contribute to differences in sNPs uptake between male-derived Caco-2 and female-derived HT-29 cells.²⁷ Overall, the inhibition patterns correlate well with previous results of sNPs uptake and mortality. This further indicates that caveolae-mediated endocytosis is a crucial pathway for sNPs internalization and cytotoxicity in cancer cells, particularly at higher concentrations.

These findings indicate that caveolae-mediated endocytosis, which M β CD inhibited, plays a crucial role in the uptake of sNPs in the tested cancer cells, with macropinocytosis (inhibited by EIPA) being less influential. The significant reduction in cytotoxicity observed when caveolae-mediated endocytosis was blocked, particularly in Caco-2 cells, underscores the importance of this pathway for sNPs uptake. The lack of significant effects in non-cancerous MCF-10A cells suggests that sNPs are internalized more by cancer cells, supporting their potential for targeted cancer therapy. Additionally, this finding supports the hypothesis that the internalization of the sNPs likely causes the killing of the cells. These findings align with previous studies demonstrating that NPs are predominantly internalized through caveolae-mediated endocytosis, while alternative pathways, such as clathrin-mediated endocytosis or macropinocytosis, contribute minimally or not at all.²⁸

Conclusions

This study demonstrates the potential of sNPs as a selective and effective anticancer therapy. The sNPs showed a significant cytotoxic effect on a range of cancer cell lines, including TR-146 buccal cancer, Caco-2 and HT-29 colorectal cancer, and MCF-7 breast cancer cells, while having minimal impact on the non-cancerous MCF-10A cells. The observed selectivity indicates that sNPs could target cancer cells without affecting normal cells, reducing the likelihood of adverse effects typically associated with conventional cancer treatments.

The flow cytometry analysis confirmed a higher uptake of sNPs by cancer cells than non-cancerous cells, supporting the hypothesis that sNPs are internalized more efficiently by cancer cells due to their enhanced endocytic activity. The evaluation of endocytosis inhibitors revealed that caveolae-mediated endocytosis plays a predominant role in sNPs uptake, with macropinocytosis also contributing to cancer cells to a lesser extent. Notably, a difference in sensitivity was observed between the Caco-2 cells (male-derived) and HT-29 cells (female-derived), with Caco-2 cells being more sensitive to sNPs. This finding is crucial for developing strategies to optimize the delivery of sNPs, potentially improving their effectiveness as targeted cancer therapeutics.

Overall, the results suggest that sNPs have strong potential as a targeted treatment option for various cancers, with further studies needed to understand the underlying mechanisms of their selective uptake and to explore their efficacy. The study's insights into endocytosis pathways provide a valuable foundation for enhancing the design and application of sNPs in future anticancer therapies.

Funding

This work was supported and funded by the Israeli Ministry of Innovation, Science, and Technology, grant no. 0004492.

Disclosure

The authors report no conflicts of interest in this work.

References

1. Rallis KS, Yau THL, Sideris M. Chemoradiotherapy in cancer treatment: rationale and clinical applications. *Anticancer Res.* **2021**;41:1–7. doi:10.21873/anticancer.14746
2. Mustapha AA, Ismail A, Abdullahi SU, et al. Cancer chemotherapy: a review update of the mechanisms of actions, prospects, and associated problems. *Biomed Nat Appl Sci.* **2021**.
3. Xia H, Hui KM. Mechanism of cancer drug resistance and the involvement of noncoding RNAs. *Curr Med Chem.* **2014**;21:3029–3041. doi:10.2174/0929867321666140414101939
4. Gould HJ, Paul D. Targeted osmotic lysis: a novel approach to targeted cancer therapies. *Biomedicines.* **2022**;10:838. doi:10.3390/biomedicines10040838
5. Gharwan H, Groninger H. Kinase inhibitors and monoclonal antibodies in oncology: clinical implications. *Nat Rev Clin Oncol.* **2016**;13:209–227. doi:10.1038/nrclinonc.2015.213
6. Keefe DMK, Bateman EH. Tumor control versus adverse events with targeted anticancer therapies. *Nat Rev Clin Oncol.* **2012**;9:98–109. doi:10.1038/nrclinonc.2011.192
7. Yuan M, Zhang G, Bai W, et al. The role of bioactive compounds in natural products extracted from plants in cancer treatment and their mechanisms related to anticancer effects. *Oxid Med Cell Longev.* **2022**;2022:1429869. doi:10.1155/2022/1429869
8. Nurkolis F, Subali D, Taslim NA, et al. *Unleashing the Potential of Marine Algae in Cancer Prevention and Treatment Through Combination of Tradition and Innovation*. Springer, Cham: Springer International Publishing; **2024**:1–30. doi:10.1007/16833_2024_212
9. Sharma R, Mondal AS, Trivedi N. Anticancer potential of algae-derived metabolites: recent updates and breakthroughs. *Future J Pharm Sci.* **2023**;9:44.
10. Saadaoui I, Rasheed R, Abdulrahman N, et al. Algae-derived bioactive compounds with anti-lung cancer potential. *Mar Drugs.* **2020**;18:197. doi:10.3390/md18040197
11. Motamedzadeh A, Rahmati-Dehkordi F, Heydari H, et al. Therapeutic potential of Phycocyanin in gastrointestinal cancers and related disorders. *mol Biol Rep.* **2024**;51:741. doi:10.1007/s11033-024-09675-3
12. Mathur M. Bioactive molecules of Spirulina: a food supplement BT. In: Mérillon J-M, Ramawat KG, editors. *Bioactive Molecules in Food*. Springer International Publishing; **2018**:1–22. doi:10.1007/978-3-319-54528-8_97-1
13. Pang QS, Guo BJ, Ruan JH. Enhancement of endonuclease activity and repair DNA synthesis by polysaccharide of Spirulina platensis. *Yi Chuan Xue Bao = Acta Genetica Sinica.* **1988**;15:374–381.
14. Ge Y, Kang Y-K, Dong L, Liu L-H, An G-Y. The efficacy of dietary Spirulina as an adjunct to chemotherapy to improve immune function and reduce myelosuppression in patients with malignant tumors. *Transl Cancer Res.* **2019**;8:1065–1073. doi:10.21037/tcr.2019.06.13
15. Drori E, Patel D, Coopersmith S, et al. Algae-based nanoparticles for oral drug delivery systems. *Mar Drugs.* **2024**;22. doi:10.3390/md22030098
16. Manual R. Cell Proliferation Kit II (XTT). *Manual.* **2005**;1–4.
17. Sasaki D, Kusamori K, Takayama Y, et al. Development of nanoparticles derived from corn as mass producible bionanoparticles with anticancer activity. *Sci Rep.* **2021**;11:22818. doi:10.1038/s41598-021-02241-y
18. Śmieszek A, Giezek E, Chrapiec M, et al. The influence of Spirulina platensis filtrates on Caco-2 proliferative activity and expression of apoptosis-related microRNAs and mRNA. *Mar Drugs.* **2017**;15:65. doi:10.3390/md15030065
19. Soror A-FS, Ahmed MW, Hassan AE, et al. Evaluation of green silver nanoparticles fabricated by Spirulina platensis phycocyanin as anticancer and antimicrobial agents. *Life.* **2022**;12. doi:10.3390/life12101493
20. Afzali M, Sadat Shandiz SA, Keshtmad Z. Preparation of biogenic silver chloride nanoparticles from microalgae Spirulina Platensis extract: anticancer properties in MDA-MB231 breast cancer cells. *mol Biol Rep.* **2024**;51:62. doi:10.1007/s11033-023-08970-9
21. Lopes-Ramos CM, Quackenbush J, DeMeo DL. Genome-wide sex and gender differences in cancer. *Front Oncol.* **2020**;10:1–17. doi:10.3389/fonc.2020.597788
22. Caserta S, Gangemi S, Murdaca G, Allegra A. Gender differences and miRNAs expression in cancer: implications on prognosis and susceptibility. *Int J mol Sci.* **2023**;24. doi:10.3390/ijms241411544
23. Lunov O, Syrovets T, Loos C, et al. Differential uptake of functionalized polystyrene nanoparticles by human macrophages and a monocytic cell line. *ACS Nano.* **2011**;5:1657–1669. doi:10.1021/nn2000756
24. Li Y, Gao X, Li Y, et al. Endocytosis: the match point of nanoparticle-based cancer therapy. *J Mat Chem B.* **2024**. doi:10.1039/D4TB01227E
25. Wang P, Shen T, Sun Y, et al. Selective killing of cancer cells by silica nanoparticles due to increased nanoparticle internalization and cellular sensitivity to oxidative stress. *J Nanopart Res.* **2023**;25:13.
26. Drori E, Rahamim V, Patel D, et al. An in vitro Caco2-based model for measuring intestinal bioadhesion comparable to ex vivo models. *Small Sci.* **2024**;5:2400461.
27. Li Y, He CL, Li WX, Zhang RX, Duan Y. Transcriptome analysis reveals gender-specific differences in overall metabolic response of male and female patients in lung adenocarcinoma. *PLoS One.* **2020**;15:1–21.
28. Wu C, Wu Y, Jin Y, et al. Endosomal/lysosomal location of organically modified silica nanoparticles following caveolae-mediated endocytosis. *RSC Adv.* **2019**;9:13855–13862. doi:10.1039/c9ra00404a

International Journal of Nanomedicine**Publish your work in this journal**

The International Journal of Nanomedicine is an international, peer-reviewed journal focusing on the application of nanotechnology in diagnostics, therapeutics, and drug delivery systems throughout the biomedical field. This journal is indexed on PubMed Central, MedLine, CAS, SciSearch®, Current Contents®/Clinical Medicine, Journal Citation Reports/Science Edition, EMBase, Scopus and the Elsevier Bibliographic databases. The manuscript management system is completely online and includes a very quick and fair peer-review system, which is all easy to use. Visit <http://www.dovepress.com/testimonials.php> to read real quotes from published authors.

Submit your manuscript here: <https://www.dovepress.com/international-journal-of-nanomedicine-journal>

Dovepress
Taylor & Francis Group